

Mask assisted Laser Percussion Drilling

C.-C. Ho^{*1}, Y.-H. Luo², Y.-J. Chang², J.-C. Hsu², and C.-L. Kuo²

¹*Department of Mechanical Engineering, National Taipei University of Technology, 1, Sec. 3,
Zhongxiao E. Rd. Taipei, Taiwan, R.O.C., 10608*

²*Department of Mechanical Engineering, National Yunlin University of Science and Technology,
123 University Road, Section 3, Douliou, Yunlin, Taiwan, R.O.C., 64002
E-mail: ccho@ntu.edu.tw*

In this work, a mask assisted laser micromachining was presented. The mask was placed upside the workpiece, and a laser beam passed through the opening hole inside the mask. Part of the plasma debris would splash on the mask through the induced shock wave when laser was striking the workpiece. Other parts of the plasma debris passed through the mask directly. The plasma debris sputtered around the top of the mask surface and avoided the plasma debris to be deposited around the drilled hole inlet. Two different camera configurations (i.e., coaxial setup and radial setup) were designed to capture the image of the plasma. By analyzing the image, the area and height of the plasma were measured at three different laser radiation energy. The hole size of mask was determined by correlated the area and height of the plasma image. Experimental results show that the processing efficiency of the laser drilling was increased to 29% and the debris height was decreased to 51% when the mask was employed to assist laser micromachining.

DOI: 10.2961/jlmn.2016.01.0008

Keywords: laser-drilled hole depth, mask assisted micromachining, measurement of plasma dimensions, laser drilling, laser machining.

1. Introduction

Laser percussion drilling of aluminum sheet finds wide applications in industry and cost competitive for a large number of holes. Laser percussion drilling has the potential to overcome the limitations by conventional methods e.g., slow processing and non-precise operation [1,2]. However, the aluminum alloy is difficult to drill by a laser due to the laser-induced plume, which reflects the optical energy and dramatically reduces the processing efficiency. It lengthens the cutting time, increasing the cost of the process and decreasing the yield.

Laser drilling utilizes the high power density to focus on a workpiece. When a laser beam impinges on a workpiece for laser drilling, laser ablation of the surface causes the melting and vaporization of the metal material during laser machining and causes the air and metallic vapor to ionize simultaneously. This evaporated material is ejected and collides with energetic electrons and result in a rapid increase in the level of ionization within the plume with the formation of the plasma. The expulsion of the ejected material during the drilling process, which subsequently sprays and re-solidifies on the material surface around the hole periphery [3]. Plume particles during laser ablation process might affect the appearance of the substrate and redeposited inside the cavity, which drastically deteriorates the quality and efficiency of laser drilling.

The review of literature shows that most of the studies are based on assisted gas solution [4,5,6] to prevent spatter during the laser drilling. During drilling processes, a coaxial assist gas jet is used in conjunction with the laser beam to increase the material ejection rate and to prevent con-

tamination of the laser optic lens surface from spatter. However, the continuously supplied gas jets cause cooling effect and the laser drilling efficiency deteriorated [7]. The rebounding gas flows carrying the molten slag and the laser-induced plume from the hole being processed may also shade the laser beam, increase the hole entrance diameter and thus reduce the processing efficiency [8]. Therefore, the use of coaxial gas jets with laser drilling suffers the problem of the molten material being over-cooled such that it cannot be ejected from the hole during drilling.

Hence, the adoption of mask device upside the workpiece is presented in this work to remove a great amount of ejected plume particles to re-solidify around the laser drilled hole. This paper investigates three different sized mask affect the performance of percussion drilling of 1 mm thick 5052 aluminum sheet using a 532 nm wavelength. Two different camera configurations (i.e., coaxial setup and radial setup) were designed to capture the image of the plasma. By analyzing the plasma image, the area and height of the plasma were measured at three different laser radiation energy. The hole size of mask was determined by correlated the area and height of the plasma image.

2. Experimental method

The configuration and experimental set-up are shown schematically in Figs. 1 and 2, respectively. A Nd:YAG pulsed laser was employed in laser drilling (Table 1), and the depth and the diameter of the laser drilling hole was inspected experimentally. The laser output was Q-switched, producing pulses of 6 ns duration and three different power levels of 1.41×10^6 , 2.45×10^6 and 3.52×10^6 W/cm², respec-

tively. The focal position of the beam was not changed during drilling. Characterization was carried out using optical microscope and three holes were measured for each processing set. The laser beam was focused with a focal length of 120 mm.

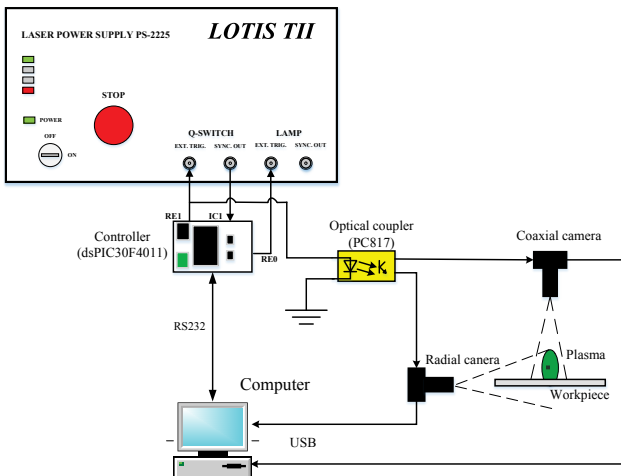


Fig. 1 Configuration for the proposed mask assisted laser percussion drilling.

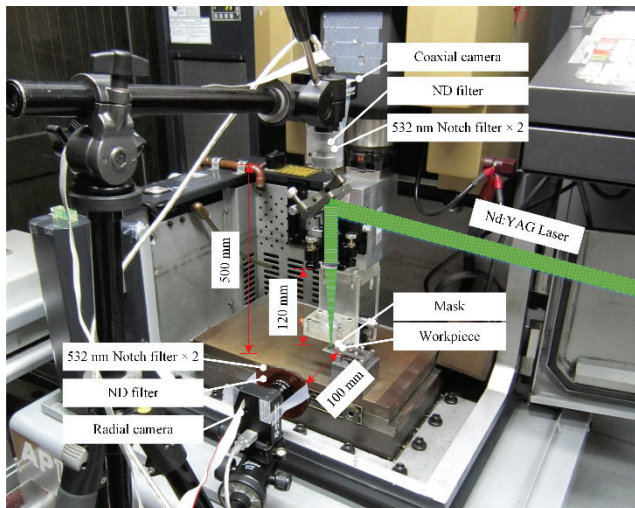
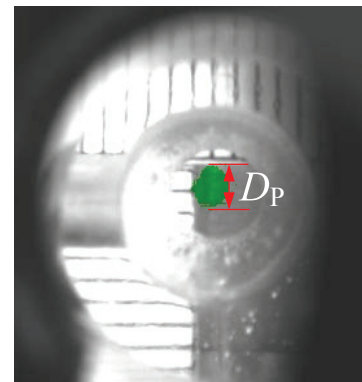


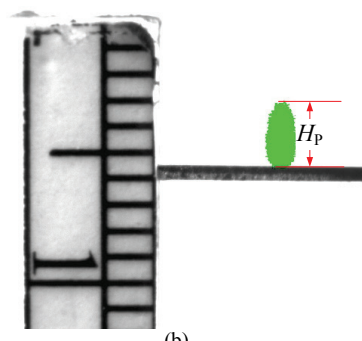
Fig. 2 Experimental setup.

Table 1 Experimental conditions.

Item	Parameter
Laser system	Nd:YAG laser
Wavelength	532 nm
Frequency	15 Hz
Laser energy	1.41, 2.45, 3.52 ($\times 10^6$ W/cm ²)
Pulse duration	6 ns
Focal length	120 mm
Material	Al 5052
Focus position	Surface
Material thickness	0.6 mm
Ambient temperature	24 °C
Ambient moisture	45 %
Mask diameter	1.25, 1.5, 2 mm
Mask gap	1 mm
Mask thickness	1 mm



(a)



(b)

Fig. 3 Plasma image captured by (a) coaxial camera; (b) radial camera.

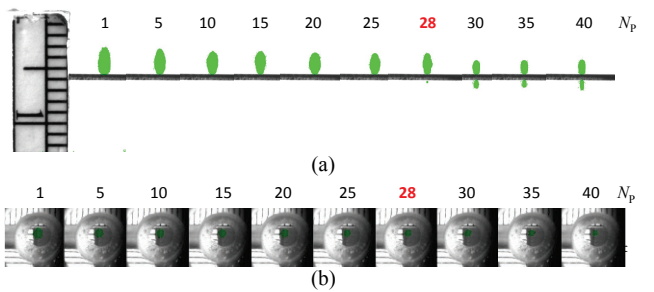


Fig. 4 A series of coaxial and radial plasma images under laser power level of 3.52×10^6 W/cm² and breakthrough occurred at pulse numbe 28.

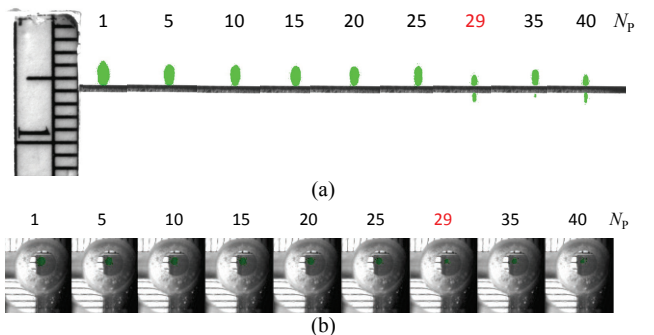


Fig. 5 A series of coaxial and radial plasma images under laser power level of 2.45×10^6 W/cm² and breakthrough occurred at pulse numbe 29.

After the surface was hit by the pulsed laser, the workpiece is heated, which causes the surface to be progressively drilled, producing a plasma plume of ionized particles ejected normally to the working site. The spatial extent of the radiation emission is obtained by the coaxial and radial camera and the total pixels in the radiation emission region of a single image frame are calculated, as shown in Fig. 3(a). During pulsed-laser drilling, several pulses are utilized for the formation of a hole. The emission of laser-

induced radiation during single-pulse drilling is detected by the camera mounted coaxially 400 mm away from the working site. Images are acquired at 15 fps and with an exposure time of 117 μ s per frame, with a picture size of 128×119 pixels. The radial camera was positioned radially 100 mm from the drilled workpiece in order to detect the moment of breakthrough and acquired the height of plasma image (i.e., H_p), as shown in Fig. 3(b). The intensity of the radiation emission is recorded as an 8-bit encoding. As a result of the pulsed laser percussion drilling, the workpiece surface is deepened for a number of pulses N_p , until the thickness of the material has been reached. A series of coaxial and radial images for a number of pulse under three different power levels of 1.41×10^6 , 2.45×10^6 and 3.52×10^6 W/cm² were displayed in Figs. 4, 5 and 6, respectively.

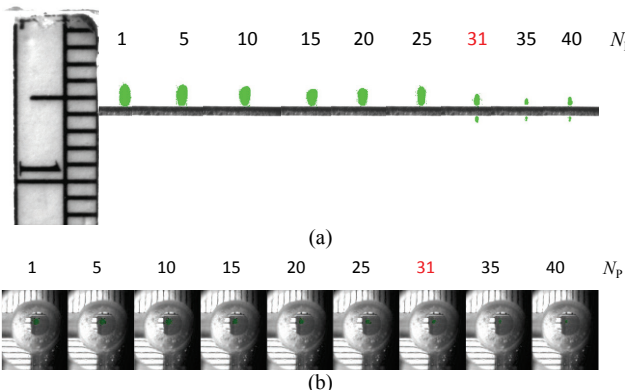


Fig. 6 A series of coaxial and radial plasma images under laser power level of 1.41×10^6 W/cm² and breakthrough occurred at pulse number 31.

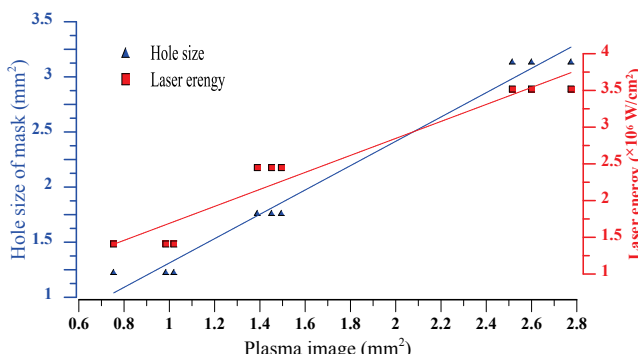


Fig. 7 Plasma image was raised as increasing the laser power with a high coefficient of (R^2) of 0.94. The hole size of mask was determined by correlated the area of the plasma image. The results reveal a high coefficient of (R^2) of 0.98.

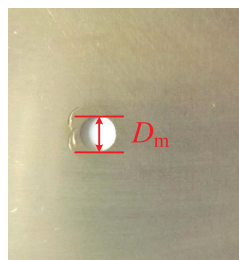


Fig. 8 The proposed mask with the different hole diameter D_m .

As depicted in Fig. 7, the plasma image acquired by the camera was raised as increasing the laser power. The results reveal a high coefficient of (R^2) of 0.94. Hence, the proposed mask was designed with a center hole within the

plate and the material is made of acrylic sheet, which is easily employed in the roll-to-roll processing to replace the heavily polluted mask, as illustrated in Fig. 8. In this approach, the laser beam is projected through the center hole of the mask and then focused onto the surface of work-piece. To avoid shielding the sputter plasma, the hole diameter of the mask (i.e., D_m) was determined by correlated the area of the plasma image. The hole diameter D_m was 1.25, 1.5 and 2 mm for power level of 1.41×10^6 , 2.45×10^6 and 3.52×10^6 W/cm² respectively. The results reveal a high coefficient of (R^2) of 0.98 between the hole size of mask and the plasma image, as depicted in Fig. 7.

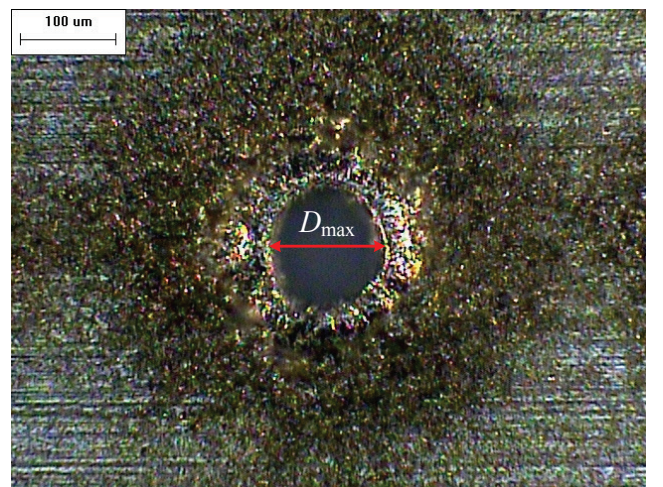


Fig. 9 The D_{\max} is the maximum diameter of the hole inlet.

3. Drilling Results and Discussion

The results of comprehensive laser drilling experiments on glass samples having dimensions of about 25 × 70 mm² showed that standard drilling without any further treatment

The drilling characteristics for holes drilled with different laser energy are reported for ambient conditions without assist-gas. In this work, the diameter of holes, and the thickness of recast were examined by optical microscopy (Olympus STM). As shown in Fig. 9, pictures of the inlet diameter D_{\max} for the hole entrance were taken; the inlet diameter for each hole was the measured maximum diameter of the hole entrance. The height of debris was measured perpendicular to the inlet surface by optical microscopy to displace the focus position from the hole entrance (Fig. 10(a)) to the ridges on top of debris flow deposits (Fig. 10 (b)). A thin circular deposited material can be observed directly in the vicinity of the hole entrance.

3.1 The influence of the laser energy

As shown in Fig. 11, the more laser energy leads to a greater inlet diameter. However, the inlet diameters were similar either with or without the mask employed during laser percussion drilling. It was well recognized that that the employed mask did not affect the inlet diameter of holes. As exhibited in Fig. 12, the debris thickness significantly decreased owing to the plasma plume produced by the laser flew in a direction perpendicular to the target surface and circulated outwards and the plume particles were deposited onto the employed mask instead of the sidewall areas of the laser drilled hole. Results revealed that the

thickness of re-deposit was reduced by employing mask configurations under different laser energies.

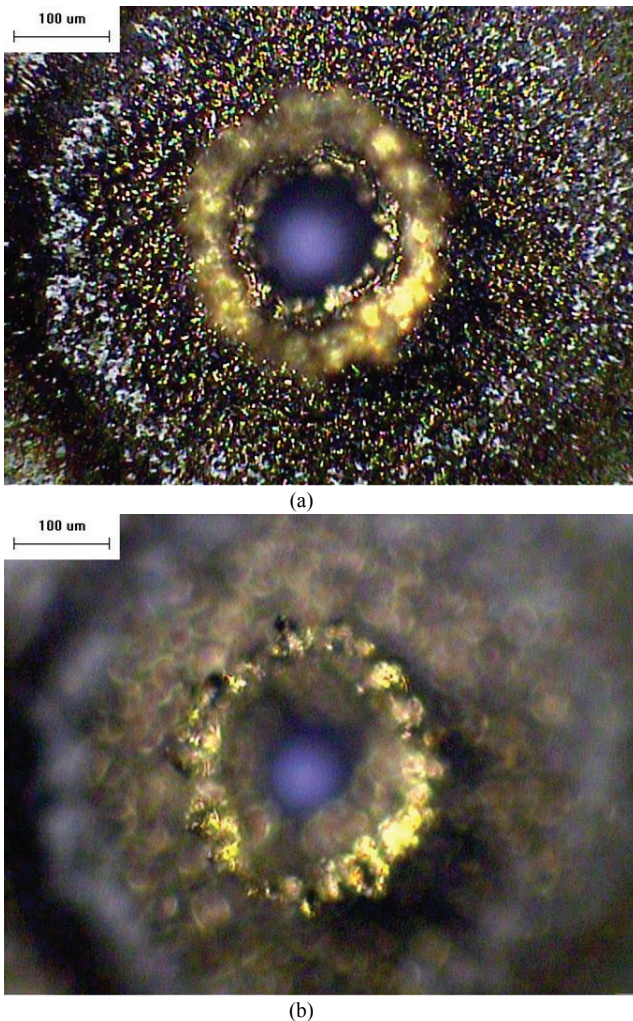


Fig. 10 The height of debris were measured by optical microscopy to displace the focus position from the hole entrance (a) to the ridges on top of de-bris flow deposits (b).

Table 2 Number of laser pulse to breakthrough the workpiece

Laser energy ($\times 10^6 \text{ W/cm}^2$)	No mask	Mask diameter D_m (mm)					
		1	1.25	1.5	2	3	4
3.52	28	25	25	24	20	25	28
2.45	29	24	22	21	22	27	28
1.41	31	27	23	25	25	31	31

3.2 The influence of the mask diameter D_m

To investigate the influence of the mask diameter D_m under same laser energy, different mask diameters D_m were employed. As shown in Table. 2, the number of breakthrough pulses could be maximally decreased to 20 for the laser energy at $3.52 \times 10^6 \text{ W/cm}^2$ under the mask diameter D_m is 2 mm. The required number of breakthrough pulses slightly increased when the mask diameter was changed. It can be seen that the much plume impurities adhere to the mask on the substrate surface for the mask diameter small than 2 mm. However, the large part of the plasma debris could not be sputtered around the top of the mask surface

for the mask diameter large than 2 mm. The situation was same for the laser energy at $2.45 \times 10^6 \text{ W/cm}^2$. The minimum breakthrough pulses were 21 under the mask diameter D_m is 1.5 mm. The lowest breakthrough pulses were 23 for the laser energy at $1.41 \times 10^6 \text{ W/cm}^2$ under the mask diameter D_m is 1.25 mm. A good agreement between plasma image correlation (Fig. 7) and the experiment (Table. 2) is found. Therefore, the drilling performance will be degraded if mask diameter is not fit the plasma size. The optimum performance in laser drilling depends on the proper selection of the mask diameter size.

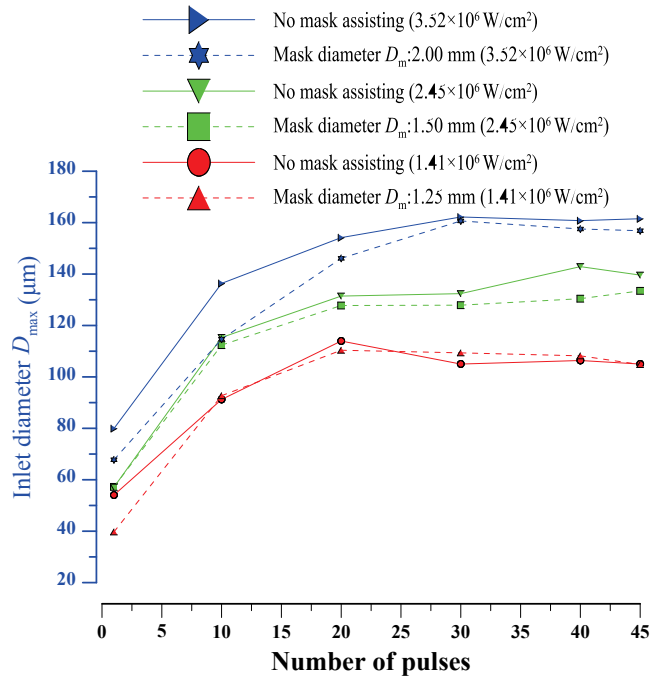


Fig. 11 The effect of mask on the diameter of debris under different laser energy.

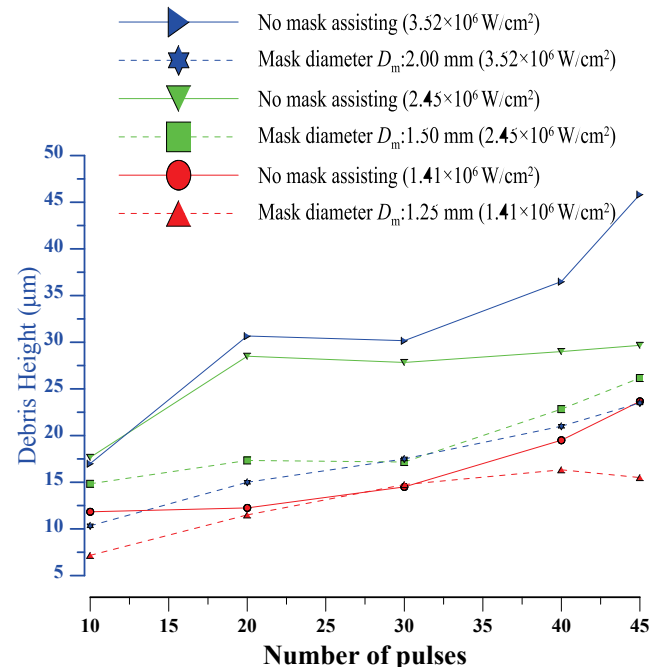


Fig. 12 The effect of mask on the height of debris under different laser energy.

3.3 The influence of the gap distance

Melt ejection is a major mechanism of material removal for the laser percussion drilling [10]. Melt particles were ejected outside the surface of the drilled hole due to the effect of recoil pressure. Therefore, the employed mask aids the drilling process by collecting the ejected melt particles. However, ejected melt particles bounce on impact when they hit the bottom of the mask surface and are deposited back onto the material surface around the hole periphery. Therefore, the decreased gap distance between the mask and the surface of the drilled hole results in the increased portion of particles to be deflected by the bottom of the mask surface. In this work, the gap distance obtained is the average of the height of plasma image over the entire drilling process.

4. Conclusions

Laser drilled holes are inherently associated with spatter deposition due to the expulsion of the ejected material from the drilling site, which subsequently solidifies and adheres on the material surface around the hole periphery. However, it is found that the plume impurities on the laser drilling surface were removed by the employed mask. By analyzing the area of the plasma image at three different laser energy. The hole size of mask was determined by correlated the area of the plasma image. Experimental results show that the processing efficiency of the laser drilling was increased to 29% and the debris height was decreased to 51% when the mask was employed to assist laser micromachining.

Acknowledgements

The work was supported by the National Science Council, Taiwan, R.O.C. MOST 103-2221-E-224-030-MY2 and 103-2622-E-224-001-CC2.

References

- [1] L. Brusberg, M. Queisser, C. Gentsch, H. Schröder, and K.-D. Lang: Phys. Procedia., 39, (2012) 548.
- [2] Y.-J. Chang, C.-L. Kuo, and N.-Y. Wang: J. Laser Micro/Nanoeng., 7, (2012) 254.
- [3] E. Kacar, M. Mutlu, E. Akman, A. Demir, L. Candan, T. Canel, V. Gunay, and T. Simmazcelik: J. Mater. Process Tech., 209, (2009) 2008.
- [4] H. Sezer, L. Li, and S. Leigh: Int. J. Mach. Tool Manu., 49, (2009) 1126.
- [5] D.-Y. Tsai and J. Lin: Opt. Laser Technol., 39, (2007) 219.
- [6] J.-C. Hsu, W.-Y. Lin, Y.-J. Chang, C.-C. Ho, and C.-L. Kuo: Int. J. Adv. Manuf. Tech., 79, (2015) 449.
- [7] K. Chen, Y. L. Yao, and V. Modi, "Gas jet-workpiece interactions in laser machining: J. Manuf. Sci. Eng., 122, (2000) 429.
- [8] D. Low, L. Li, and A. Corfe: Appl. Surf. Sci., 154, (2000) 689.
- [9] A. Khan, S. Celotto, L. Tunna, W. O'Neill, and C. Sutcliffe: Opt. Lasers Eng., 45, (2007) 709.
- [10] K. Voisey, S. Kudesia, W. Rodden, D. Hand, J. Jones, and T. Clyne: Mater. Sci. Eng., A, 356, (2003) 414.

(Received: June 10, 2015, Accepted: January 17, 2016)